Internal electronic structure of adatoms on Fe(110) and Fe(100) surfaces: A low-energy Li^+ scattering study

Y. Yang,[1] Z. Sroubek,[2] and J. A. Yarmoff[1,*]
[1]*Department of Physics, University of California, Riverside, California 92521, USA*
[2]*Czech Academy of Sciences, URE, Chaberská 57, Prague 8, Czech Republic*
(Received 12 August 2003; revised manuscript received 27 October 2003; published 29 January 2004)

The neutralization of 400–3000 eV $^7Li^+$ ions scattered from clean and adsorbate-covered Fe(110) and Fe(100) surfaces was measured with time-of-flight spectroscopy. Li singly scattered from bromine, iodine, and cesium adatoms has a consistently larger neutral fraction than that for scattered from substrate sites. This suggests that the local electrostatic potential directly above these adatoms is reduced from that of the clean substrate. The neutral fraction of Li scattered from halogen adatoms is surprising in that it decreases as the emission angle moves off-normal, yet increases in the usual manner for cesium and silver adatoms. This indicates that the charge distribution associated with a halogen adsorbate is nonuniform, most likely due to internal polarization. A semiquantitative theoretical analysis shows that a nonuniform internal electron density would give rise to the observed behavior. The polarization of halogen adatoms is likely responsible for anomalous work function changes observed previously. Alkali-ion scattering is shown to be an effective tool for detecting the internal electronic structure of an adatom.

DOI: 10.1103/PhysRevB.69.045420 PACS number(s): 68.43.−h, 68.49.Sf, 79.20.Rf, 73.90.+f

I. INTRODUCTION

Halogens have a remarkable variety of applications in electrochemistry, lamps, etching, dry processing, and surface preparation and are used as catalytic poisons and promoters. Because of their technological significance, halogen adsorption and reactions have attracted much attention in the surface science community.[1–3] Despite the amount of work devoted to this subject, however, the local electronic structure and the nature of halogen–transition-metal bonding are still unclear. In addition, based on simple electronegativity considerations, halogen adsorption would be expected to increase the surface work function. It has been found, however, that the work function actually decreases upon halogen adsorption on a number of transition-metal surfaces.[4–8] Several empirical and theoretical models[4,5,9,10] have been proposed to explain this phenomenon, but their reliability has not been tested because of lack of information on the microscopic electronic structure. In addition, all attempts of using a single dipole layer to explain the anomalous work function behavior have been unsuccessful.[10]

As a surface analytical method, low-energy ion scattering has the advantage of extreme surface specificity.[11] In addition to surface composition and structure analysis, neutralization during low-energy ion scattering can be employed to probe the local charge states of adsorbates on surfaces, especially when alkali ions are used as the projectiles.[12–14] This is because the alkali *ns* valence levels overlap the metal Fermi level so that resonant charge transfer (RCT) dominates over the other charge transfer processes.[15] RCT only involves outer shell electrons so that the charge exchange probabilities are strongly influenced by the local surface electronic environment.

Charge exchange in low-energy alkali-ion scattering from alkali-covered metal surfaces has been studied by several groups.[12–14,16–19] All these results indicate that the local inhomogeneity in the electrostatic potential of the adsorbate layer plays an important role in the charge transfer process. In particular, the neutralization probabilities of the particles scattered from different surface sites, which were determined for Li^+ scattering from alkali-covered Al and Ni, carry quantitative information on the local electrostatic potential[12–14] (LEP). A satisfactory agreement between the experimental results and *ab initio* theory was achieved by introducing variations in the energy and width of the projectile level corresponding to the LEP around the alkali adatom.[20,21]

In contrast, there have been few studies of alkali-ion scattering from halogen-covered metal surfaces. In a recent Letter,[22] we showed results of low-energy Li^+ scattering from iodine adsorbed on iron, which suggest that the internal polarization of the adatom plays an important role in the neutralization process. More comprehensive experiments are carried out in the present paper, and the effects of different incident ion energies and various halogen (I, Br) and other adsorbates (Cs, Ag) on the neutralization of scattered Li are investigated. We show that the charge exchange process is dominated by the LEP change induced by the adsorbates when relatively high incident beam energies and large scattering angles are used. Independent of the coverage, the neutralization probability of the particles scattered from a halogen adatom is always larger than that from the substrate, which suggests a lower potential directly above the halogen adatom. The neutral fraction of Li scattered from the halogen adsorbate deceases as the exit angle increases with respect to the surface normal, which is in contrast to the more usual behavior for cesium and silver adsorbates. These data can be explained by considering a large polarization effect within an adsorbed halogen, and show that alkali-ion scattering is sensitive to the internal charge distribution of a surface adatom.

II. EXPERIMENTAL PROCEDURE

The experiments were performed in an ultrahigh vacuum (UHV) chamber with a base pressure of about 5×10^{-11} Torr. Prior to introducing the iron single crystal samples into the UHV chamber, they were treated in a furnace at 800 °C under a constant flow of pure hydrogen gas for about 6 weeks to remove the sulfur and oxygen impurities embedded in the bulk.[23] The samples were cleaned *in situ* in the UHV chamber with cycles of 1-keV Ar^+ sputtering and annealing at 700–750 °C. The cleanliness of the surfaces was checked with Auger electron spectroscopy (AES) employing a cylindrical mirror analyzer (Perkin-Elmer), which indicated no evidence of carbon or oxygen. The overlayer symmetries of the surfaces were determined with low-energy electron diffraction (LEED). Sharp (1×1) patterns were repeatedly obtained for clean Fe(110) and Fe(100).

Iodine and bromine were deposited from solid-state electrochemical cells based on Ag halide pellets.[24,25] The cells were operated between 140 and 160 °C. After each deposition, the surface composition was checked with AES, which showed no silver or oxygen impurities from the cells. The halogen exposures are reported in μA min, i.e., the product of the operating current and exposure time. It is estimated that a 10 μA min exposure approximately corresponds to one I_2 or Br_2 molecule impinging on each surface atom. Cs deposition was performed using a well-outgassed getter (SAES) with the sample held at room temperature. Ag (α, 99.9985%) was evaporated from a W filament (Mathis).

Changes in the work function induced by halogen, Cs, and Ag adsorption were determined by the energy shift of the secondary-electron cutoff measured with a hemispherical electrostatic analyzer (Comstock). The secondary electrons were generated by impinging a 200-eV electron beam onto the sample.

Time-of-flight (TOF) spectra were collected with equipment similar to that described elsewhere.[12] The $^7Li^+$ ions were produced from a thermionic emitter ion gun (Kimball Physics). The energy spread of the incident $^7Li^+$ beam was less than 0.2%. The beam was deflected across a 1.0-mm^2 aperture to produce 40-ns pulses at a rate of 80 kHz. The scattered ions and neutrals were detected by a microchannel-plate (MCP) array after traveling a total path length of 0.57 m. Parallel to the flight path, a set of $\sim 5 \times 5$-mm^2 deflection plates were positioned on opposite sides of the scattered beam. ''Total yield'' spectra were collected with both plates held at ground, while ''neutrals only'' spectra were collected by placing +200 V on one plate to deflect the scattered ions. The entrance to the MCP detector was held at ground to ensure that ions and neutrals were collected with equal efficiency.

III. RESULTS

Representative total yield and neutrals only TOF spectra are shown in Fig. 1 for 2.5-keV $^7Li^+$ backscattered from Fe(110) following iodine and bromine adsorption. The single scattering peaks (SSP's) are sharp features that result from

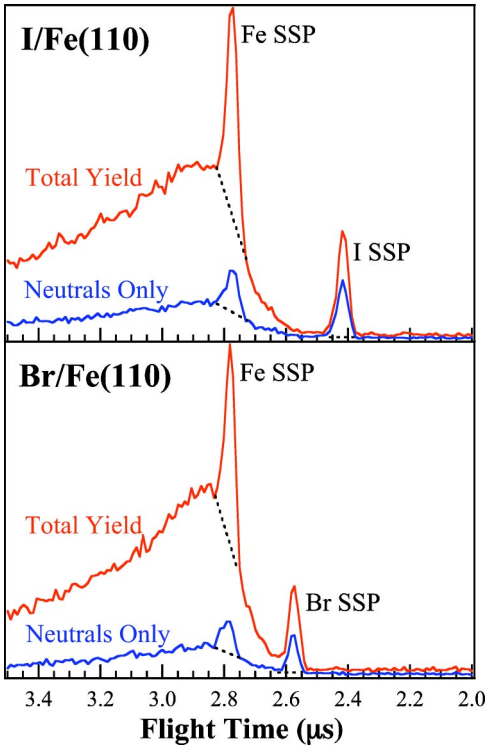

FIG. 1. (Color online) TOF spectra of the total and neutral yields collected at a 168° scattering angle for normally incident 2.5 keV $^7Li^+$ scattered from iodine-adsorbed and bromine-adsorbed Fe(110). The corresponding I_2 and Br_2 exposures are 100 and 200 μA min, respectively.

binary elastic scattering from a single surface atom or adatom, while the background signal arises from Li projectiles that have undergone multiple collisions. The Fe SSP's are well resolved from the background in all spectra, and the I and Br SSP's are well separated from their respective Fe SSP's so that the neutral fractions could be independently monitored for single scattering from the different sites. The neutral fractions were determined by dividing the integrated area of the neutrals only SSP by that of the total yield SSP. The areas were calculated following the subtraction of a linear background (typical backgrounds are shown by dashed lines in Fig. 1).

Note that the calculated neutral fraction is rather insensitive to the background subtraction procedure because the neutral fractions of the substrate SSP and the multiple scattering background underneath it have nearly identical values. In fact, the neutral fractions calculated for the Fe SSP by taking the ratio of the neutral to total yields in a ± 20-eV window centered about the Fe SSP maximum without any background subtraction fall within the uncertainty range of the values determined with background subtraction. For the adsorbate SSP's, the background subtraction is clear cut because of their simple shape and the absence of any significant multiple scattering signal underneath the peaks.

A. Energy dependence of the neutral fraction

Previous studies have shown that the neutralization probability of alkali ions scattered from a clean metal sur-

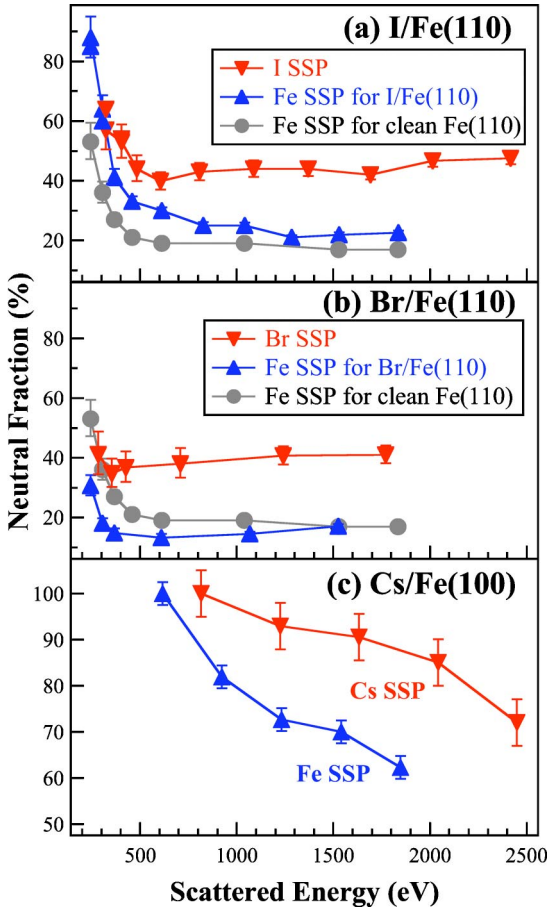

FIG. 2. (Color online) Neutral fractions versus final energy for normally incident Li particles scattered at 168° from (a) I-adsorbed Fe(110), (b) Br-adsorbed Fe(110), and (c) Cs-adsorbed Fe(100). Both iodine and bromine exposures are 200 μA min. The Cs-induced work function change is -1.1 eV. The neutral fraction error analysis assumes that the uncertainty in the calculated SSP area equals the square root of the area. Note that in some cases the markers representing the data points are larger than the error bars. Also shown in (a) and (b) are the neutral fraction of the Fe SSP's for clean Fe(110) as a function of scattered Li energy.

face depends on the component of the outgoing velocity that is perpendicular to the surface.[26,27] Thus, for a given scattering angle, the neutralization probability changes with the incident ion energy. As the energy decreases, the neutralization process becomes more adiabatic, which in the present case produces more neutrals since the work function of Fe (4.6–5.1 eV) is smaller than the ionization potential of Li (5.39 eV). We carried out series of measurements for halogen-adsorbed Fe surfaces using incident beam energies ranging from 0.4 to 3.0 keV to investigate the energy dependence of neutralization in the presence of surface adsorbates.

The neutral fractions of the I, Br, and Fe SSP's for a fixed exit angle of 12° from the surface normal are plotted in Figs. 2(a) and 2(b) against the final energy of the scattered Li. The scattered energy, rather than the incident energy, is used here since the neutralization is determined along the exit trajectory, and different amounts of energy are lost in scattering from the iron and halogen sites. Similar experiments were performed for clean Fe(110), and these data are included for comparison. The results show that the neutral factions of the I and Br SSP's vary with the scattered Li energy in a similar way. At low scattered energy, the I (or Br) and Fe neutral fractions are relatively large and comparable to each other. As the energy increases, the neutral fractions of the halogen and Fe SSP's both decrease, but more importantly, they diverge. The neutral fraction of the halogen (I or Br) SSP is significantly larger than that of Fe SSP for all scattered energies above $\sim$300 eV.

To determine whether the energy dependence is the same for both negatively and positively charged adsorbates, neutral fraction measurements versus incident energy were performed for Cs-covered Fe(100), and the results are shown in Fig. 2(c). The energy dependences of the neutral fractions have the same overall trend as with halogens. For large scattered energies, the neutral fractions of Cs and Fe SSP's are very different from each other. As the energy decreases, the two neutral fraction curves both increase and gradually approach each other.

These results indicate that the neutral fraction measurement is sensitive to the local adatom-induced LEP change only for relatively high scattered (and correspondingly high incident) ion energies. At low energies, the charge transfer process approaches the adiabatic limit, and the neutral fraction measurement does not reveal inhomogeneities in the potential close to the surface. Accordingly, for the remainder of the experiments reported here, the incident Li^+ energy was kept at the relatively high energy of 2.5 keV. For single scattering at 168° from Fe, Br, and I atoms, the corresponding scattered Li energies are 1.5, 1.8, and 2.0 keV, respectively. Note in Figs. 2(a) and 2(b) that for final energies above 1.0 keV, the variations in the neutral fraction curves are relatively small. Thus, differences in energy due to scattering from different atomic sites do not affect the results.

B. Exposure dependence of the neutral fraction and work function

Figure 3(a) shows the work function ϕ and the ratio of the AES I(MNN)/Fe(LMM) peaks as functions of iodine exposure on Fe(110). The AES data show that the iodine coverage increases monotonically for exposures below 200 μA min. The linear increase of the I coverage in the low-exposure range suggests a constant initial sticking coefficient. The rate of increase slows somewhat for higher exposure, although the exposures used here are not sufficient to reach saturation. The work function decreases with increasing iodine exposure up to $\sim$100 μA min, after which it increases back to its clean surface value. The evolution of the LEED pattern suggests that the behavior of the work function is surface-structure related. When the iodine exposure is below 20 μA min, no significant change in the substrate (1×1) LEED pattern is observed. At an iodine exposure of about 50 μA min, a sharp $c(1\times3)$ pattern is obtained. As the iodine exposure is increased to 200 μA min, the LEED pattern transforms into a $c(1\times5)$ pattern. This is qualitatively consistent with the previous reports.[28,29] The iodine adatoms occupy different surface sites as the adsorbate coverage is

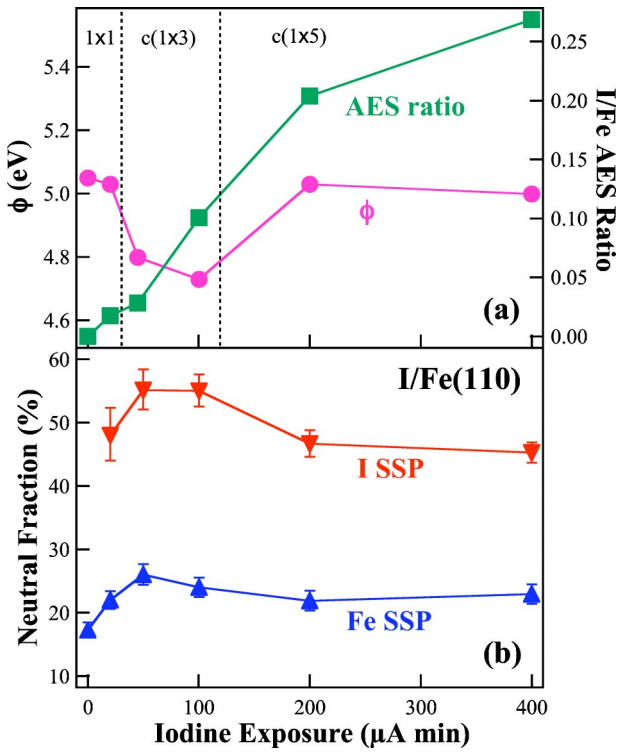

FIG. 3. (Color online) (a) Work function (ϕ) and ratio of the AES I(MNN)/Fe(LMM) peaks as functions of iodine exposure on Fe(110). Also indicated are the surface structures obtained by LEED. The work function value for clean Fe(110) was taken as 5.05 eV (Ref. 44). (b) Neutral fractions of the I and Fe SSP's versus iodine exposure. The $^7Li^+$ beam was incident along the surface normal, and the scattering angle was 168°.

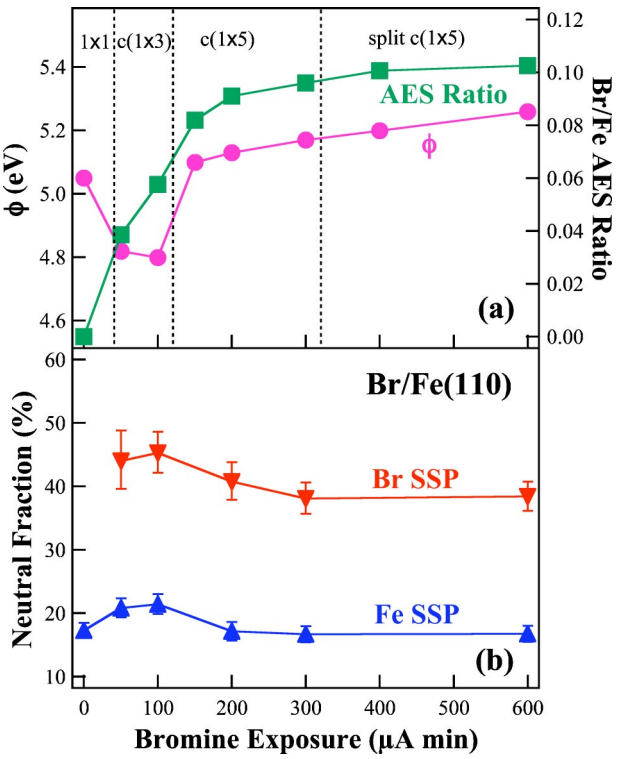

FIG. 4. (Color online) (a) Work function (ϕ) and ratio of the AES Br(LMM)/Fe(LMM) peaks as functions of bromine exposure on Fe(110). Also indicated are the surface structures obtained by LEED. The work function value for clean Fe(110) was taken as 5.05 eV (Ref. 44). (b) Neutral fractions of the Br and Fe SSP's versus bromine exposure. The $^7Li^+$ beam was incident along the surface normal, and the scattering angle was 168°.

increased, which leads to the changes in the LEED patterns and the detailed shape of the work function curve.

The neutral fractions of the I and Fe SSP's are shown in Fig. 3(b) as a function of I_2 exposure. They are nearly constant over the range of exposures employed, but do display broad maxima in the exposure range of 50–100 μA min. The shape of the work function curves are roughly ''mirrored'' in the neutral fraction curves, which is consistent with the prediction of the RCT model that the neutral fraction goes in the opposite direction as the work function change.[15] A surprising feature of the data, however, is that the I SSP neutral fractions are considerably larger than those of the Fe SSP over the entire iodine exposure range.[22]

Similar results are found for bromine adsorption on Fe(110), as shown in Fig. 4. The Br(LMM)/Fe(LMM) AES ratio rapidly increases for exposures below 200 μA min, also indicating a constant initial sticking coefficient. Thereafter, the ratio levels out, indicating that the sticking coefficient drops dramatically. Note that halide island growth could occur at the largest bromine exposures.[3] Upon Br adsorption, the LEED pattern changes continuously. Accompanying the surface structure change, ϕ goes through a minimum at a Br exposure of about 100 μA min. The variations in the neutral fractions of the Br and Fe SSP's follow the same trends as the I/Fe(110) system. Similar to I/Fe(110), the most significant feature of Fig. 4 is that the neutral fraction of the Br SSP is larger than that of Fe SSP at all exposure levels. Following the largest Br exposures, the neutral fractions of the Br and Fe SSP's stabilize, but at relatively smaller values than those for I-covered Fe(110).

We have also measured neutralization probabilities for Li^+ scattered from iodine and bromine adsorbed on Fe(100). Figure 5 shows the neutral fractions of the I, Br, and Fe SSP's along with the work function curves, plotted against the halogen exposure. Also indicated are the surface-structure symmetries obtained by LEED, which are consistent with previous results.[30,31] The work function increases upon both I and Br adsorption on Fe(100), with the increase for Br/Fe(100) being somewhat larger. All of the neutral fractions are nearly constant over the exposure range, but the neutral fractions of the halogen SSP's decrease slightly as more halogen is adsorbed. The halogen neutral fractions are much larger than those of iron over the entire coverage range, similar to halogen-adsorbed Fe(110).

IV. DISCUSSION

To gain insight into the charge transfer process at halogen-adsorbed surfaces, both the macroscopic work function change induced by the halogens and the modification of the LEP around each individual halogen adatom need to be considered. For large-angle scattering, however, the projec-

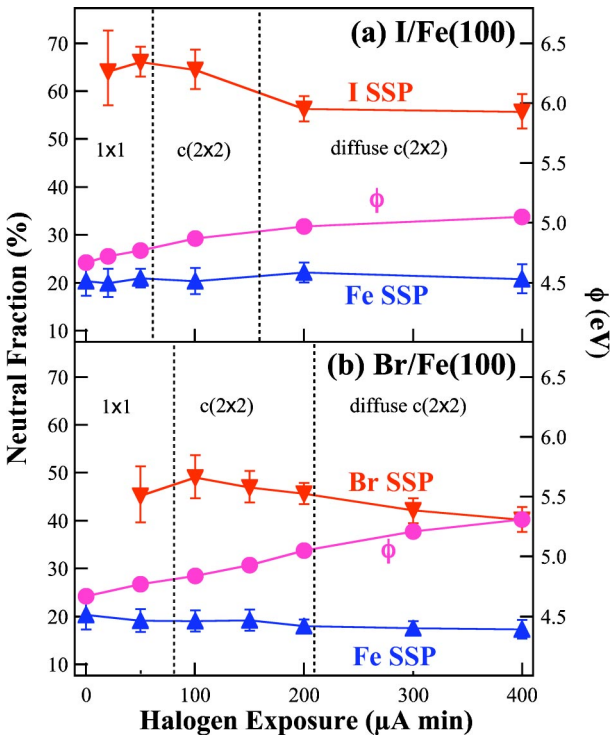

FIG. 5. (Color online) (a) Neutral fractions of the I and Fe SSP's and work function (ϕ) versus I_2 exposure on Fe(100). (b) Neutral fractions of the Br and Fe SSP's and work function (ϕ) versus Br_2 exposure on Fe(100). The $^7Li^+$ beam was incident along the surface normal, and the scattering angle was 168°. The surface structures obtained by LEED are also indicated. The work function value for clean Fe(100) was taken as 4.67 eV (Ref. 45).

tile only probes a very small region of the surface so that the outcome is usually dominated by the local properties.[18,32] In addition, the relatively high energies used here further enhance the sensitivity of ion scattering to the local electronic structure.

At first, it may appear straightforward to explain the high neutral fraction for scattering from the halogen by considering the increased electron density at the halogen site. But photoemission shows that the occupied halogen-adsorbate states lie well below the Fermi level.[33] Because of the small Li ionization potential, resonant electron transfer between the halogen-induced states and the Li level is rather unlikely. In fact, in all cases the neutralizing electron comes from the metal valence band. Thus, it is the local potential at the halogen site that makes the dramatic difference in the neutralization rate and not the density of electronic states.

Based on a simple consideration of the surface charge distribution, the negatively charged halogen atom, along with its image charge in the substrate, should create an inward-pointing dipole. As a result, the potential should be larger in the vicinity of the halogen adatom as compared to a bare metal site. But the large neutral fractions of the halogen SSP's suggest that the LEP is actually lower at the halogen sites. In addition, a negative halogen-induced dipole cannot explain the work function decrease observed on Fe(110) and many other transition-metal surfaces.[4–8]

Several explanations for the work function decrease had been previously proposed, with subsurface penetration of the halogen leading to an outward-pointing dipole being the most common.[4,7] For single-crystal surfaces, however, it has been found that halogens do not penetrate the lattice and instead are most often positioned above the outermost substrate atoms at well-defined sites.[33–36] Furthermore, it might be expected that halogen penetration would be enhanced on the more open (100) surfaces, but instead these surfaces generally show the expected increase in work function.[6,37] Penetration also fails to explain why larger work function decreases are caused by iodine adsorption, as opposed to other halogens,[8] since penetration should be reduced due to the larger size of the iodine atom. The notion that the halogen adatom is internally polarized, thus leading to a combination of inward and outward dipoles, is consistent with the known adsorption sites and can explain both the ion scattering and work function data.[10,22]

A. Internal polarization of halogen adsorbates

Internal polarization of halogens in the vicinity of a surface is not a new idea. Realizing the difficulty of relating the electronegativity of halogen adsorbates to the work function change, Pettersson and Bagus[38] pointed out that halogen adatoms on metal surfaces could polarize to a large extent. Their cluster-model study showed that the polarization of both the halogen anion and the metal dramatically reduced the dipole moment from that given by the unpolarized surface dipole. Thus, a change in work function is not simply a measure of the adsorbate ionicity. Based on density-functional calculations, Wu and Klepeis[10] proposed a multidipole model that considers the internal charge distribution of a polarizable halogen adatom. Their results indicated that the charge redistribution could be treated as the sum of three dipole layers. The outermost dipole results from the polarization of the halogen adatom by the field of the metallic surface and points outwards; the second, which is the expected inward-pointing dipole, is due to the electronic charge transfer from the metal to the adsorbate; the third arises from the effect of Smoluchowski smoothing in the near-surface region of the metal. The overall work function change is thus determined by competition between the negative contributions of the first and third dipoles and the positive contribution of the second dipole.

The multidipole model suggests that although the halogen adatom carries an overall negative charge, this charge is not uniformly distributed around the halogen ion core (see Fig. 6 for a sketch). Such a region of electron depletion above the halogen adatom is clearly visible in the electron density contour plots of Ref. 39 shown for Cl adatoms on metal surfaces, although this detail was not mentioned by the authors themselves. As shown in these plots, a positive image charge resides directly beneath the negatively charged halogen adatom. As a result, the negative charge surrounding the halogen ion core is attracted toward its image charge in the surface, leaving a region of positive charge above the adatom.

This comprehensive picture of halogen adsorbates is adopted here to explain the neutral fractions observed in Li^+ scattering.[22] When backscattered alkali ions exit nearly

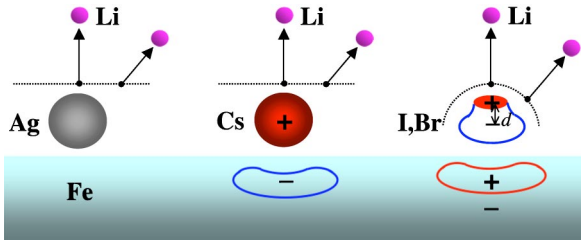

FIG. 6. (Color online) Schematic diagram illustrating the electron density associated with neutral (Ag), positively charged alkali (Cs), and negatively charged halogen (I, Br) adsorbates on an Fe metal surface. The arrows show the outgoing trajectories of scattered Li, and dotted lines are drawn to indicate the surface along which charge formation occurs, as used in the calculations. This diagram shows how these various charge distributions influence the potential experienced by the projectiles. Note that in estimating the local electrostatic field induced by the adatom, we neglect the contribution of the image charges shown in the figure.

perpendicular to the surface, the particles ''feel'' the potential directly above the scattering site. Since there is an attractive potential directly above the polarized halogen due to the outermost dipole, the LEP at the top of a halogen adatom is lower than that near an Fe surface atom. The attractive potential lowers the energy level of the projectile, thereby increasing the neutralization probability. As a result, the neutral fractions of the halogen SSP's are larger than those of the Fe SSP's.

B. Comparison with alkali adsorbates

The important role that an inhomogeneous LEP plays in charge exchange was previously shown by Li-ion scattering from alkali-covered metal surfaces.[12,13] At low alkali coverage, the neutralization probability of the alkali SSP is also much larger than that of the metal SSP. An alkali adatom donates its valence electron to the surface and is adsorbed as a positive ion (as illustrated in Fig. 6), thus creating an outward-pointing dipole and lowering the potential in the vicinity of the adatom. Consequently, the neutralization probability is larger for ions scattered from the alkali sites.

In the sense of the ''outermost'' dipole field, halogen adsorbates have similar effects on charge exchange as alkali, but their differences become apparent as the adsorbate coverage increases. As the coverage of alkali increases, the adsorbates interact, which leads to a depolarization of the individual dipoles and a reduction of the inhomogeneities in the LEP.[20,40] As a result, the difference between the neutral fractions of the alkali and metal SSP's become smaller. At the highest coverages, the LEP approaches that of a uniform dipole sheet and becomes nearly homogeneous. Accordingly, the neutral fractions of the alkali and metal SSP's become nearly identical.[12–14]

For halogen adsorption, however, the polarization of the halogen atom (the attractive potential of the first dipole) is very localized at the top of adatom. Since the difference between the halogen and substrate neutral fractions is nearly constant as the coverage changes, the internal polarization that leads to the outermost dipole must be a local phenomenon that is not affected by neighboring adatoms. As the halogen exposure increases, the interaction between the adatoms may cause the second and third dipoles to become less polarized, but this apparently does not affect the neutral fractions measured at normal exit angles.

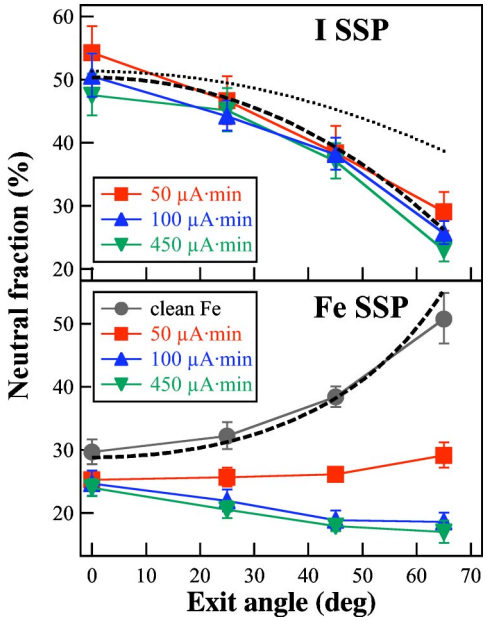

FIG. 7. (Color online) (a) Neutral fractions of the I SSP versus the exit angle (with respect to surface normal) for Li scattered at 155° from iodine-covered Fe(100). (b) Neutral fractions of the Fe SSP versus the exit angle for Li scattered from clean and iodine-covered Fe(100). The measurements were carried out for three iodine exposures, which were 50, 100, and 450 μA min, respectively. The semiquantitative theoretical estimations (see text) are shown as the dotted and dashed lines.

C. Angular dependence of the neutral fraction

For backscattering along a near-normal exit trajectory, the potential induced by the first halogen dipole plays a key role in neutralization. If the charge transfer were to occur more toward the side of the halogen atom, however, the repulsive potential induced by the second dipole should become more prevalent. This can be accomplished by utilizing a more grazing exit angle, as illustrated by the tilted arrow of Fig. 6. Hence, if the notion of internal polarization were correct, a reduced neutral fraction for scattering from the halogen site would be expected for a glancing exit trajectory.

This effect was indeed observed for I-covered Fe surfaces when the sample was tilted with respect to the TOF detector.[22] In Fig. 7(a), the neutral fractions of the I SSP as a function of the exit angle following three different iodine exposures are shown by the solid symbols. It is quite surprising that neutralization would decrease as the exit angle becomes more grazing, as it is in conflict with any model for charge transfer that considers the surface potential to be isotropic. For a polarized halogen adatom, however, the LEP changes sign as the angle is swept across the spherical sur-

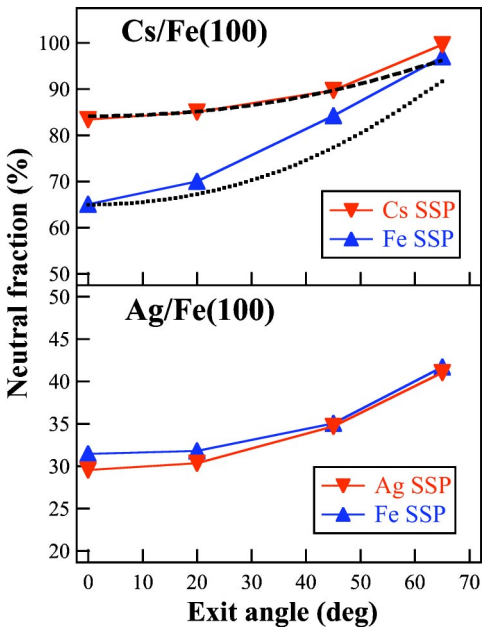

FIG. 8. (Color online) Neutral fractions of $^7Li^+$ singly scattered from adsorbate and substrate sites shown as functions of the exit angle for (a) Cs-covered and (b) Ag-covered Fe(100). The corresponding Cs- and Ag-induced work function changes were -1.0 eV and $+0.18$ eV, respectively. The scattering angle was 160°. The semiquantitative theoretical estimations (see text) are shown as the dashed lines.

face that is probed by the exiting ion, as illustrated in Fig. 6. Thus, an increase in the exit angle can give rise to a reduction in the neutralization probability. Since the reduction in neutralization is nearly the same for various iodine coverages, it appears as though any effects of adatom-adatom interactions on the internal electronic distributions are minimal.

The angular dependence of the Fe SSP is also affected by iodine exposure. Following a small exposure (50 μA min), the Fe SSP neutral fraction increases with exit angle, although not as strongly as with the clean surface. Following larger iodine exposures, however, the Fe SSP neutral fraction decreases somewhat as the exit angle increases. This is because the exiting Li has a high probability of interaction with nearby iodine adatoms following the large exposures. Thus, a Li particle originally scattered from an Fe surface atom may encounter the delocalized repulsive potential of the negative iodine (the second dipole) on its way out, thereby reducing its neutralization probability.

We also investigated the angular dependence of the Li^+ neutralization rate for Cs- and Ag-adsorbed Fe(100), as shown in Fig. 8. The coverage of adsorbates was calibrated by both AES and work function measurements, and was kept low in order to make the LEP as inhomogeneous as possible. In all cases, the neutral fractions increase monotonically for more grazing exit angles, as expected. Alkali adatoms form single outward-pointing dipoles at the surface, so that the scattered Li does not experience a change in the sign of the potential as the exit angle changes. The attractive potential at the Cs site causes the neutral fraction of the Cs SSP to be larger than that of the Fe SSP for near-normal angles, and they gradually approach each other for more glancing exit trajectories. For Ag adatoms, the neutral fractions of the adsorbate and substrate SSP's have nearly the same values at all angles. Ag atoms on metal surfaces form largely covalent bonds that are accompanied by very small charge displacements.[41] Thus, the surface dipole induced by a Ag adatom is insignificant and there is minimal difference in the LEP between the Ag and Fe sites, which gives rise to similar neutralization rates.

D. Semiquantitative theoretical estimate

In order to clarify our interpretation of the experimental results, we outline a semiquantitative theoretical estimate of the influence of the adatom-induced electrostatic potential on the neutralization probability of Li^+ ions scattered from surface adsorbates. This analysis shows that the internal electronic structure of the halogen adatoms does lead to the observed neutralization behavior.

The dynamics of resonant charge exchange is usually modeled with the Newns-Anderson Hamiltonian.[42,43] Typically, the charge formation process is described by the energy and virtual width of the valence level of the scattered projectile, and the time dependence of the level energy and width produces nonadiabatic excitations in the atom-surface system. While the energy of the valence level is mostly governed by the surface electrostatic potential, the width of the valence level is determined by electron exchange between the atom and the metal surface. The width depends, for a given scattered particle, upon the substrate local density of states (LDOS) at the Fermi level projected onto the scattering site. In general, it is the width of the valence level, and not its energy, that determines the distance above the surface at which charge formation takes place. Under conditions in which the substrate can be represented by a free electron gas, this distance is laterally independent and the relevant velocity component of the scattered particle is normal to the surface. This would also be the case for an isolated adsorbate on a surface if it could be represented by a slowly varying LEP immersed in the free electron gas and the adsorbate did not protrude above the surface. If the adsorbate were situated above the surface, we can assume that the LDOS follows the contour of the impurity, although the LDOS may not be laterally independent in this case.

Under the approximation of a slowly varying LEP, the nonadiabatic neutralization N can be well described by a simple analytical solution of the Newns-Anderson Hamiltonian,

$$N = \left[1 - \exp\left(\frac{-C(\Delta E + \delta E)}{v_r}\right)\right] \times 100\%, \qquad (1)$$

where ΔE is the potential difference between the substrate Fermi level and the projectile ionization level, and δE is the potential modification induced by the adsorbate. Both ΔE and δE are taken at the location where the charge exchange occurs. The parameter C depends on the electronic structure of the substrate-projectile system, and v_r represents the relevant velocity component of the scattered particle. The char-

acteristic dependence of N on δE and v_r, as given by Eq. (1), is analytically obtained from the Anderson Hamiltonian whether the ionization level is far below the Fermi level at all times or the ionization level is above the Fermi level at the surface and dips below the Fermi level during the emission, although the physical content of the product $C\Delta E$ is different in these two cases. Thus, Eq. (1) is also expected to hold for intermediate cases. We have checked the applicability of Eq. (1) for the analysis of our data by comparing, in certain instances, the N obtained from Eq. (1) to the N obtained by a complete solution of the Newns-Anderson Hamiltonian in the independent particle picture[15,42,43] and found them to be comparable.

For scattering from a clean metal surface, the neutralization probability depends mainly on the normal velocity component of the outgoing particle[12,43] as mentioned above. We neglect the parallel velocity effect as it was found to be small in Li scattering.[26] Using this assumption, the velocity v_r in Eq. (1) can be expressed as $v\cos\theta$, where v is the total velocity and θ is the exit angle with respect to the surface normal. By using the measured N value of the clean Fe surface for $\theta=0$, $C\Delta E/v$ in Eq. (1) is found to be 0.34. Assuming that $C\Delta E/v$ is constant, the neutral fraction calculated from Eq. (1) is plotted versus the exit angle by the dashed line in Fig. 7(b), which closely follows the experimental result for clean Fe.

The angular dependence of the Fe substrate SSP neutral fraction in the presence of Cs, as shown in Fig. 8(a), can be interpreted in a similar manner by again assuming that the potential is laterally smooth. Due to Cs deposition, the work function decreases by 1.1 eV and N of the Fe SSP at $\theta=0$ increases from 30% to 65%. This corresponds to an increase from $C\Delta E/v=0.34$ for clean Fe to $C\Delta E'/v=1.05$ for Cs-covered Fe. The resulting θ dependence of the Fe SSP neutral fraction, as predicted by Eq. (1), is shown in Fig. 8(a) by a dotted line. The calculated line matches the experimental data reasonably well.

In scattering from the Cs adsorbates, the neutralization is influenced by both the change of the work function, i.e., the change of ΔE to $\Delta E'$, and the change of the local potential. Both of these changes are caused by the positive charge of the Cs atom. The value of the work function is laterally independent, whereas the local quantity δE can be considered in its simplest form as the local potential induced by a positive charge lying above the surface, i.e., $\delta E(\mathrm{Cs}) = e^*(\mathrm{Cs})/r$, where $e^*(\mathrm{Cs})$ is the effective positive charge of Cs and r is the distance from the adatom to the point where charge exchange takes place. If we use the assumption that the charge exchange occurs at a fixed distance l from the surface, i.e., $r=l/\cos\theta$, then the term $C\delta E(\mathrm{Cs})/(v\cos\theta)$ is nearly angularly independent and we take it as a constant. By fitting the value of N for the Cs SSP at $\theta=0$, we obtain a value of 0.80 for the constant. The dashed line in Fig. 8(a) indicates the corresponding calculated angular dependence.

For iodine adsorbates, the experimental evidence indicates that the adatom needs to be considered as an outward dipole positioned above the surface, rather than merely as a negative point charge. The quantity δE therefore has a dipole character, i.e., $\delta E(I)=[p^*(\mathrm{I})/r^2]\cos\theta$. $p^*(\mathrm{I})$ is the electrical dipole moment of the iodine adatom and is equal to $e^*(\mathrm{I})d$, where $e^*(\mathrm{I})$ is the effective negative charge of iodine and d is the dipole length. r is again the distance from the adatom to the point where the charge exchange takes place, which should be on the order of the Li $2s$ electron radius. We consider the iodine adatom to be protruding above the surface, as indicated in Fig. 6. Unlike the Cs adatom, however, the LEP around a halogen adatom is strongly corrugated. This is due to the fact that the outward-pointing dipole composed of the positive region at the top of the adatom and the negative charge associated with the bulk of the adatom lies well above the surface. Thus, it is expected that the LEP would change quickly with the exit angle. The most reasonable assumption in this case is that ionization occurs at a fixed distance from the adatom, i.e., r is constant as suggested by the dotted line surrounding the halogen adatom in Fig. 6. The value of $Cp^*(\mathrm{I})/vr^2$ can then be deduced from the neutral fraction data at $\theta=0$ in Fig. 7(a). Using this value and assuming that $C\Delta E/v$ is equal to the value found for clean Fe, the angular dependence of N can be estimated, as is shown in Fig. 7(a) by the dotted line. Although the trend is correct, the decrease of N with θ is not as great as in the experimental data.

In the real system, a negative imbalance of the iodine dipole charge is very likely to occur, as suggested schematically by the shape of the halogen adatom in Fig. 6. This can be taken into account by modifying $\delta E(\mathrm{I})$ to $[p^*(\mathrm{I})/r^2]\cos\theta - \delta e^*(\mathrm{I})/r$, where $\delta e^*(\mathrm{I})$ represents the magnitude of the charge imbalance. Under this assumption, we get a better agreement with the experiment, as shown by the dashed line in Fig. 7(a). A fitting procedure yields $Cp^*(\mathrm{I})/vr^2=0.69$ and $C\delta e^*(\mathrm{I})/vr=0.29$. Assuming that the effective charge of iodine is equal to that of Cs, i.e., $e^*(\mathrm{I})=e^*(\mathrm{Cs})$, the length ratio d/r is 86% and the charge imbalance is 36%. These are physically reasonable results in which the dipole approximation is satisfied, because d is indeed smaller than r.

Although this theoretical description is approximate, the good agreement with the experimental data indicates that an iodine dipole on the surface with a charge imbalance produces a neutral fraction that decreases as the exit angle becomes more grazing. Thus, the theoretical analysis has verified our hypothesis concerning the origin of the angular dependence of the I SSP neutral fraction.

V. CONCLUSIONS

The neutralization of Li^+ scattered from Fe(110) and Fe(100) surfaces was measured as a function of the incident ion energy, adatom charge and coverage, and the exit angle. We found that the sensitivity of ion scattering to the LEP change above different scattering sites can be greatly enhanced by employing a relatively high incident energy and large scattering angle. Iodine and bromine adsorption initially deceases the work function of Fe(110) and increases the work function of Fe(100). While the detailed shape of the halogen-coverage dependence of the scattered Li neutral fraction can be correlated to the halogen-induced work function change, the considerably larger neutral fractions of Li

singly scattered from the halogen sites are caused by the presence of a lower potential directly above a halogen adatom. As the exit beam moves off-normal, the neutral fraction of Li scattered from iodine adsorbates decreases. This is in contrast to cesium and silver adsorbates where the neutral fractions increase for more glancing exit trajectories. These angular dependences are attributed to the nonuniform charge distribution around the halogen adatoms induced by internal polarization, which is further verified by a semiquantitative theoretical analysis. Our results confirm the internal polarization of halogen adatoms on metal surfaces and demonstrate that it likely causes the anomalous work function changes observed upon halogen adsorption. Overall, we showed that low-energy ion scattering yields unique information on the adatom electrostatic potential.

ACKNOWLEDGMENTS

The authors would like to thank Dr. Christine J. Wu for the helpful discussions, and the National Science Foundation (Grant No. CHE-0091328) for financial support.

*Author to whom correspondence should be addressed. Email address: yarmoff@ucr.edu

[1] W. C. Simpson and J. A. Yarmoff, Annu. Rev. Phys. Chem. **47**, 527 (1996).
[2] H. F. Winters and J. W. Coburn, Surf. Sci. Rep. **14**, 161 (1992).
[3] P. A. Dowben, CRC Crit. Rev. Solid State Mater. Sci. **13**, 191 (1987).
[4] D. L. Fehrs and R. E. Stickney, Surf. Sci. **17**, 298 (1969).
[5] C. W. Jowett and B. J. Hopkins, Surf. Sci. **22**, 392 (1970).
[6] Z. Stott and H. Hughes, Vacuum **31**, 487 (1981).
[7] J. S. Foord and R. M. Lambert, Surf. Sci. **138**, 258 (1984).
[8] S. K. Jo and J. M. White, Surf. Sci. **261**, 111 (1992).
[9] E. Shustorovich, Surf. Sci. Rep. **6**, 1 (1986).
[10] C. J. Wu and J. E. Klepeis, Phys. Rev. B **55**, 10 848 (1997).
[11] H. Niehus, W. Heiland, and E. Taglauer, Surf. Sci. Rep. **17**, 213 (1993).
[12] C. B. Weare and J. A. Yarmoff, Surf. Sci. **348**, 359 (1996).
[13] C. B. Weare, K. A. H. German, and J. A. Yarmoff, Phys. Rev. B **52**, 2066 (1995).
[14] J. A. Yarmoff and C. B. Weare, Nucl. Instrum. Methods Phys. Res. B **125**, 262 (1997).
[15] J. Los and J. J. C. Geerlings, Phys. Rep. **190**, 133 (1990).
[16] J. J. C. Geerlings, L. F. T. Kwakman, and J. Los, Surf. Sci. **184**, 305 (1987).
[17] G. A. Kimmel, D. M. Goodstein, Z. H. Levine, and B. H. Cooper, Phys. Rev. B **43**, 9403 (1991).
[18] L. Q. Jiang, Y. D. Li, and B. E. Koel, Phys. Rev. Lett. **70**, 2649 (1993).
[19] Q. B. Lu, R. Souda, D. J. O'Connor, and B. V. King, Phys. Rev. Lett. **77**, 3236 (1996).
[20] A. G. Borisov, G. E. Makhmetov, D. Teillet-Billy, and J. P. Gauyacq, Surf. Sci. **375**, L367 (1997).
[21] D. G. Goryunov, A. G. Borisov, G. E. Makhmetov, D. Teillet-Billy, and J. P. Gauyacq, Surf. Sci. **401**, 206 (1998).
[22] J. A. Yarmoff, Y. Yang, and Z. Sroubek, Phys. Rev. Lett. **91**, 086104 (2003).
[23] V. S. Smentkowski, C. C. Cheng, and J. T. Yates Jr., Langmuir **6**, 147 (1990).
[24] N. D. Spencer, P. J. Goddard, P. W. Davies, M. Kitson, and R. M. Lambert, J. Vac. Sci. Technol. A **1**, 1554 (1983).
[25] W. K. Wang, W. C. Simpson, and J. A. Yarmoff, Phys. Rev. Lett. **81**, 1465 (1998).
[26] G. A. Kimmel and B. H. Cooper, Phys. Rev. B **48**, 12164 (1993).
[27] B. Rasser, J. N. M. van Wunnik, and J. Los, Surf. Sci. **118**, 697 (1982).
[28] D. R. Mueller, T. N. Rhodin, and P. A. Dowben, J. Vac. Sci. Technol. A **4**, 1518 (1986).
[29] D. Mueller, Y. Sakisaka, and T. Rhodin, J. Vac. Sci. Technol. A **2**, 1018 (1984).
[30] R. G. Jones and D. L. Perry, Surf. Sci. **88**, 331 (1979).
[31] P. A. Dowben and R. G. Jones, Surf. Sci. **88**, 348 (1979).
[32] K. A. H. German, C. B. Weare, P. R. Varekamp, J. N. Andersen, and J. A. Yarmoff, Phys. Rev. Lett. **70**, 3510 (1993).
[33] D. R. Mueller, T. N. Rhodin, Y. Sakisaka, and P. A. Dowben, Surf. Sci. **250**, 185 (1991).
[34] R. G. Jones, Prog. Surf. Sci. **27**, 25 (1988).
[35] L. Q. Wang, Z. Hussain, Z. Q. Huang, A. E. Schach von Wittenau, D. W. Lindle, and D. A. Shirley, Phys. Rev. B **44**, 13711 (1991).
[36] M. Saidy, K. A. R. Mitchell, S. A. Furman, M. Labayen, and D. A. Harrington, Surf. Rev. Lett. **6**, 871 (1999).
[37] M. Grunze and P. A. Dowben, Appl. Surf. Sci. **10**, 209 (1982).
[38] L. G. M. Pettersson and P. S. Bagus, Phys. Rev. Lett. **56**, 500 (1986).
[39] M. Scheffler and C. Stampfl, in *Handbook of Surface Science*, edited by K. Horn and M. Scheffler (Elsevier Science, Amsterdam, 2000), Vol. 2, p. 285.
[40] H. P. Bonzel, A. M. Bradshaw, and G. Ertl, *Physics and Chemistry of Alkali Metal Adsorption* (Elsevier, Amsterdam, 1989).
[41] M. Mayer, G. Pacchioni, and N. Rosch, Surf. Sci. **412–413**, 616 (1998).
[42] A. Blandin, A. Nourtier, and D. W. Hone, J. Phys. I **37**, 369 (1976).
[43] J. B. Marston, D. R. Andersson, E. R. Behringer, B. H. Cooper, C. A. DiRubio, G. A. Kimmel, and C. Richardson, Phys. Rev. B **48**, 7809 (1993).
[44] G. Pirug, G. Brodén, and H. P. Bonzel, Surf. Sci. **94**, 323 (1980).
[45] D. R. Lide, in *CRC Handbook of Chemistry and Physics* (CRC, New York, 2001).